Sensorless Control of a Ferrite PM Assisted-Synchronous Reluctance Machines by Using Sliding Mode Observer and High Frequency Signal Injection

Zhiwei Zhang[1], Libing Zhou[1]
[1]*School of Electrical and Electronic Engineering, Huazhong University of Science and Technology, 1037 Luoyu Road, 430074, Wuhan, China*
d200877200@hust.edu.cn

***Abstract*—This paper presents sensorless control of ferrite permanent magnet-assisted synchronous reluctance machines (FPMA-SynRM) over wide speed range by using sliding mode observer (SMO) and high frequency signal injection. The basic equation of sliding mode observer will be derived based on dynamic model of PMSynRM. In the study, the equivalent of EMF-based SMO is proposed to estimate rotor position at medium and high speed range. The principles of high frequency signal injection, digital signal processing and rotor polarity identification is also analysed. Finally, the theoretical analysis have been verified with the experiments and the results obtained show that the resolution of estimated position signal can meet requirements of some industrial drive applications.**

***Index Terms*—Sensorless; ferrite permanent magnet; synchronous reluctance machine; sliding mode observer; high frequency signal injection.**

I. INTRODUCTION

The conventional rare-earth interior permanent magnet synchronous machine was popular in industrial drive applications, particularly in electric vehicle traction systems, over several decades due to its high torque density, high efficiency, wide constant power range, *etc.* [1]. However, the high cost, limited resources and unstable supply of rare-earth permanent magnet are challenging issues. Additionally, in high speed operation range, the dominant component of stator current is negative *d*-axis demagnetized current to weaken the flux linkage produced by stronger rare earth permanent magnet, which increase the risk of demagnetization of rare-earth permanent magnet.

Ferrite permanent magnet-assisted synchronous reluctance machine is the combination of synchronous reluctance machine and ferrite-permanent magnet-excited synchronous machine. The torque density and power factor of pure synchronous reluctance machines are relatively poor. In order to enhance torque density of pure synchronous reluctance machines, the low cost ferrite permanent magnets can be inserted into rotor lamination to improve torque density and power factor. Compared to conventional rare earth permanent magnet machines, the reluctance torque component is dominant in ferrite permanent magnet-assisted synchronous reluctance machine. It is said that the FPMA-SynRM will be a good candidate for various industrial drive applications, particularly for next generation electric vehicle of hybrid electric vehicle traction. [2]–[5].

In high performance vector controlled ferrite permanent magnet-assisted synchronous reluctance machine -based dive systems, the rotor position signal is needed to achieve field orientation and speed close-loop control. Various position sensors, such as optical encoder, resolver, low cost Hall Effect sensor, are used to detect rotor position signal. However, these position sensor increase cost, machine size, and other issues. Sensorless control of AC drive has received much more attentions. Back-EMF estimation-based sensorless control strategy is only effective one in medium and high speed region. However, in low speed region and standstill, it is so difficult to estimate because the magnitude of back-EMF is very small or zero. Another rotor estimation scheme, which is so-called high frequency signal injection, can be used in low speed region and standstill [6], [7].

This paper presents sensorless control of ferrite permanent magnet-assisted synchronous reluctance machines over wide speed range by using sliding mode observer and high frequency signal injection. The topology and feature of proposed ferrite permanent magnet-assisted synchronous reluctance machines will be introduced firstly. Sliding mode observer based on equivalent EMF theory will be designed. In low and zero speed regions, high frequency signal injection is proposed to estimated rotor position. Additionally, rotor polarity will be identified by utilizing magnetic saturation effect. Finally, sensorless control scheme over wide speed range for proposed ferrite permanent magnet-assisted synchronous reluctance machines will be verified by experiments.

II. PROPOSED FPMA-SYNRM

Figure 1 shows conventional pure synchronous reluctance machines and proposed ferrite permanent magnet-assisted synchronous reluctance machines. The saliency difference or ratio plays a key role for reluctance torque production in synchronous reluctance machines. In order to enhance the

Manuscript received 21 December, 2015; accepted 24 May, 2016.

saliency ratio, the axially-laminated rotor has been proposed for maximizing reluctance torque contribution [8]. However, the disadvantages of axially-laminated rotor are high eddy current rotor losses and relatively complicated construction process. Another popular rotor structure is multi-barriers-based transversally-laminated rotor. In this rotor, the single or multi-layer flux barriers are necessary to decrease d-axis reluctance. Furthermore, in order to enhance torque density and power factor, the low cost ferrite magnets can be inserted into outer rotor lamination.

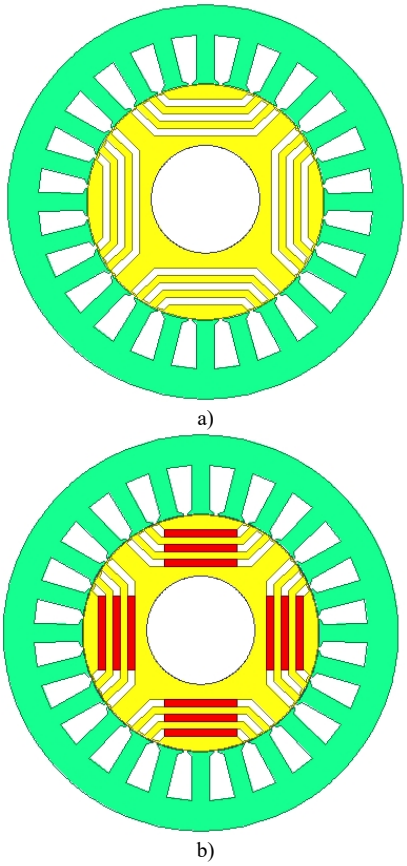

Fig. 1. Cross-sections of synchronous reluctance machines and proposed ferrite permanent magnet-assisted synchronous reluctance machines: (a) synchronous reluctance machines; (b) ferrite permanent magnet-assisted synchronous reluctance machines.

III. DESIGN OF SMO

The dynamic equation of proposed ferrite permanent magnet-assisted synchronous reluctance machine can be expressed as in (1)

$$\vec{v}_s = (\boldsymbol{R}_s + p\boldsymbol{L}_s)\vec{i}_s + \vec{e}_s, \tag{1}$$

where $\vec{v}_s = \begin{bmatrix} v_\alpha \\ v_\beta \end{bmatrix}$, $\vec{i}_s = \begin{bmatrix} i_\alpha \\ i_\beta \end{bmatrix}$, $\vec{e} = \begin{bmatrix} e_\alpha \\ e_\beta \end{bmatrix} = \omega\lambda_m \begin{bmatrix} -\sin\theta \\ \cos\theta \end{bmatrix}$.

The resistance matrix can be expressed as in (2)

$$\boldsymbol{R}_s = \begin{bmatrix} R_s & 0 \\ 0 & R_s \end{bmatrix}, \tag{2}$$

where v_α, v_β, i_α, i_β, e_α, e_β are voltage, current, and back-EMF component in stationary reference frame, respectively, λ_m is flux linkage due to permanent magnet, R_s is phase resistance.

For proposed PMA-SynRM, the inductance matrix can be

$$\boldsymbol{L}_s = \begin{bmatrix} L_0 + L_1\cos 2\theta & L_1 \sin 2\theta \\ L_1 \sin 2\theta & L_0 - L_1 \cos 2\theta \end{bmatrix}, \tag{3}$$

where $L_0 = \dfrac{L_d + L_q}{2}$, $L_1 = \dfrac{L_d - L_q}{2}$.

For classical surface-mounted permanent magnet machines, the inductance matrix can be simplified as

$$\boldsymbol{L}_s = \begin{bmatrix} L_s & 0 \\ 0 & L_s \end{bmatrix}. \tag{4}$$

By using equivalent EMF theory, the voltage equation can be modified as [8]

$$\begin{bmatrix} v_\alpha \\ v_\beta \end{bmatrix} = \begin{bmatrix} R_s & \\ & R_s \end{bmatrix}\begin{bmatrix} i_\alpha \\ i_\beta \end{bmatrix} + p\begin{bmatrix} L_q & \\ & L_q \end{bmatrix}\begin{bmatrix} i_\alpha \\ i_\beta \end{bmatrix} + \begin{bmatrix} e'_\alpha \\ e'_\beta \end{bmatrix}. \tag{5}$$

The state variable equation is

$$p\begin{bmatrix} i_\alpha \\ i_\beta \end{bmatrix} = \frac{1}{L_q}\begin{bmatrix} v_\alpha \\ v_\beta \end{bmatrix} - \frac{R_s}{L_q}\begin{bmatrix} i_\alpha \\ i_\beta \end{bmatrix} - \frac{1}{L_q}\begin{bmatrix} e'_\alpha \\ e'_\beta \end{bmatrix}. \tag{6}$$

The sliding mode observer equation is

$$\begin{bmatrix} \hat{i}_\alpha \\ \hat{i}_\beta \end{bmatrix} = \frac{1}{L_q}\begin{bmatrix} v_\alpha \\ v_\beta \end{bmatrix} - \frac{R_s}{L_q}\begin{bmatrix} i_\alpha \\ i_\beta \end{bmatrix} - \frac{K_{smo}}{L_q}\begin{bmatrix} sign(\hat{i}_\alpha - i_\alpha) \\ sign(\hat{i}_\beta - i_\beta) \end{bmatrix}, \tag{7}$$

where $\hat{i}_\alpha$, $\hat{i}_\beta$ are estimated current, K_{smo} is observer gain.

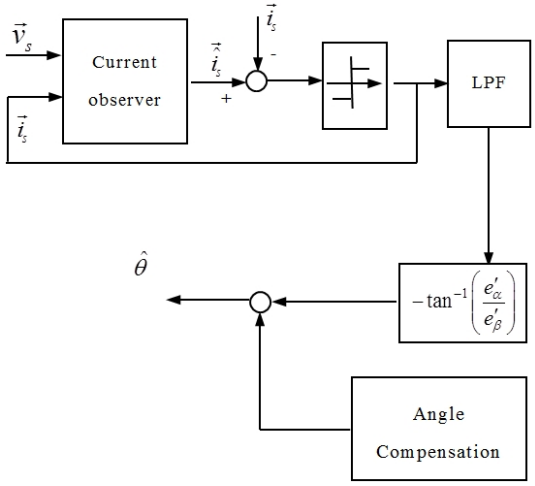

Fig. 2. Block diagram of sliding mode observer for proposed PMA-SynRM.

The estimated current will converge to actual measured current when the estimation error reaches the sliding surface. Figure 2 shows the block diagram of sliding mode observer for proposed permanent magnet-assisted synchronous machines. Voltage and current vector are the input of sliding mode - based current observer. The error of estimated current and measured current will be forced by a sign function. A simple low pass filter is employed to exact the alpha and beta component of equivalent back-EMF. Finally, and inverser tan function is needed to calculated the vector angle. Obviously, the estimated theta should be compensated due to the phase delay.

IV. ROTATING HF SIGNAL INJECTION

Sliding mode observer is suitable for medium and high speed region. However, in low speed region and standstill, the back-EMF is too small or zero. It is very difficult to estimate by sliding mode observer. The high frequency signal injection is an effective way to estimate the rotor position in low speed region and standstill by utilizing saliency effect.

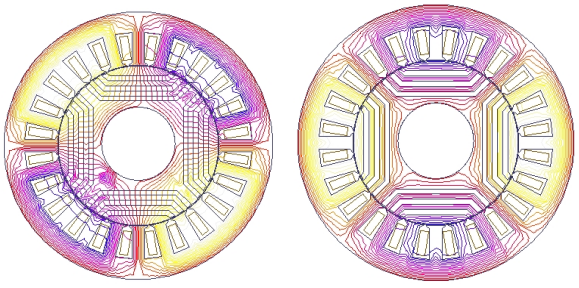

a) b)

Fig. 3. Flux line distribution of proposed PMA-SynRM excited by d-axis and q-axis current: (a) d-axis excitation; (b) q-axis excitation.

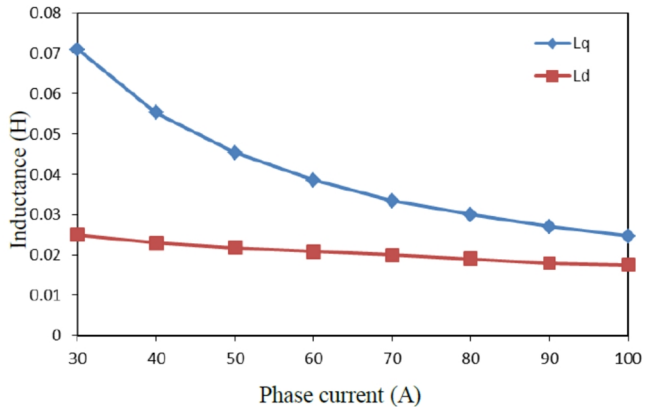

Fig. 4. D-axis and q-axis inductance of proposed PMA-SynRM.

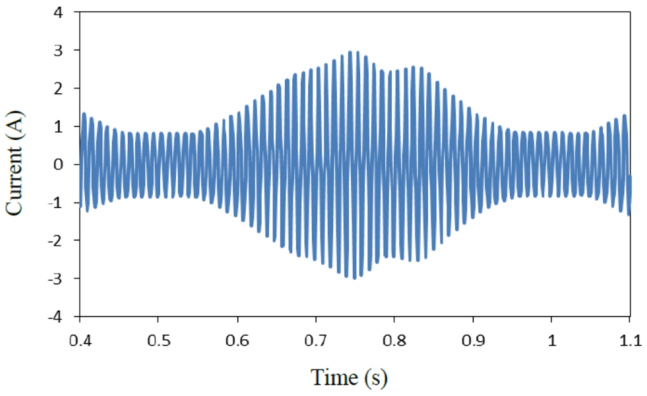

Fig. 5. Phase current waveform under high frequency voltage excitation.

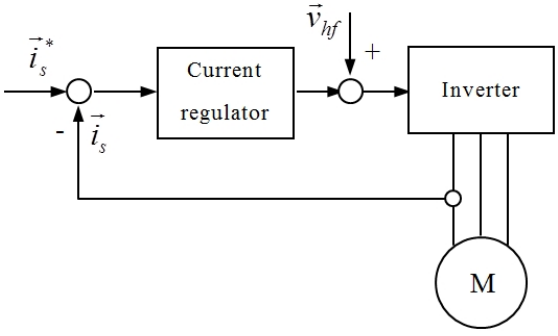

Fig. 6. Block diagram of sliding mode observer for proposed PMA-SynRM.

Figure 3 shows finite element method-predicted flux line distribution excited by stator *d*-axis and *q*–axis current. Figure 4 shows the *d*-axis and *q*-axis inductance variation with magnitude of phase current. It can be seen that the *d*-axis inductance is lower than *q*-axis inductance, which resulted in saliency effect. Figure 5 shows phase current waveform when high frequency voltage injected. It can be seen that the magnitude of phase current is variable due to saliency effect of proposed ferrite permanent magnet-assisted synchronous reluctance machines.

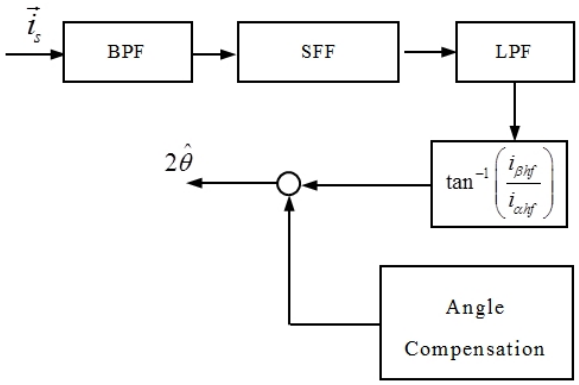

Fig. 7. Block diagram of digital signal processing for proposed FPMA-SynRM.

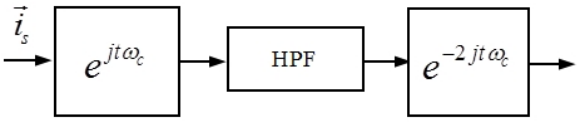

Fig. 8. Block diagram of synchronous frame filter.

Rotating high frequency signal injection method can be divided into voltage signal injection and current signal injection. High frequency current signal injection scheme means that the additional signal is injected before current regulator. However, this scheme suffers from the bandwidth limitation of current regulator. As a result, voltage signal injection is more popular. The block diagram of rotating high frequency voltage signal injection was shown in Fig. 6. The high frequency voltage signal is injected after current regulator. The current response will be measured and demodulated by advanced digital signal processing technology.

The phase current under high frequency voltage excitation can be expressed as in (8) [9]

$$i_{hf}(t) = \frac{-jV_{hf}}{2\omega_c L_{ld} L_{lq}}[(L_{ld} + L_{lq})e^{j\omega_c t} + \\ +(L_{ld} - L_{lq})e^{j(-\omega_c + 2\omega_r)t}] = \\ = i_{hf-p} + i_{hf-n}. \quad (8)$$

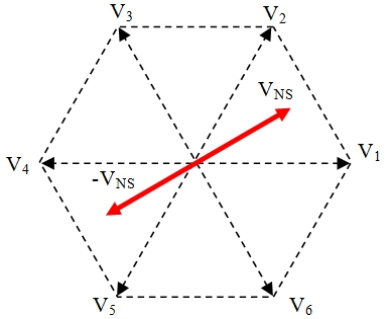

Fig. 9. Space vector of three phase inverter.

From the equation, the current response include positive and negative component. It should be pointed out that only negative component of high frequency component include rotor position information.

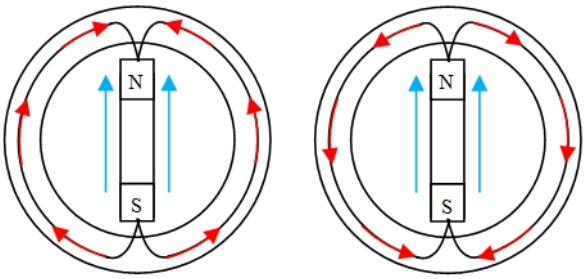

(a) (b)

Fig. 10. Flux direction generated by both permanent magnet and stator winding.

Figure 7 shows block diagram of digital signal processing. After high frequency voltage injection, the current response has three components, including fundamental component, high frequency component, and switching frequency component. The fundamental and switching frequency components can be filtered out by band pass filter (BPF). The positive component of high frequency current can be filtered out by synchronous frame filter. The block diagram of synchronous frame filter was shown in Fig. 8. Then, the rotor position can be estimated by (9)

$$2\hat{\theta}_r = \tan^{-1}\left(\frac{i_{\beta hf}}{i_{\alpha hf}}\right). \quad (9)$$

It should be pointed out that phase compensation is needed because of a delay caused by filter.

V. Rotor Polarity Identification

After rotor position estimation by using high frequency signal injection, the polarity of rotor permanent magnet is still unknown. In this section, the north and south pole of rotor permanent magnet will be identified based on magnetic saturation effect of proposed ferrite permanent magnet synchronous reluctance machines.

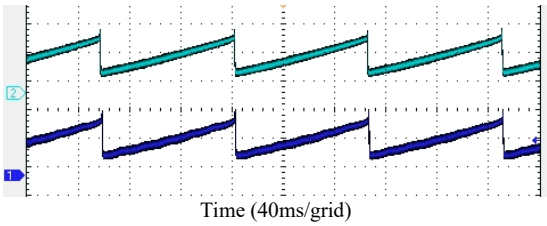

Time (40ms/grid)

Fig. 11. High frequency injection-based experimental results (1: estimated result of high frequency injection, 2: measured result of position sensor).

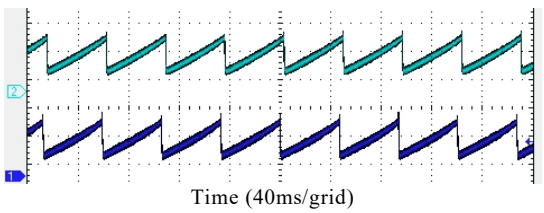

Time (40ms/grid)

Fig. 12. Sliding mode observer-based experimental results (1: estimated result of sliding mode observer, 2: measured result of position sensor). Horizontal axis: 40ms/grid.

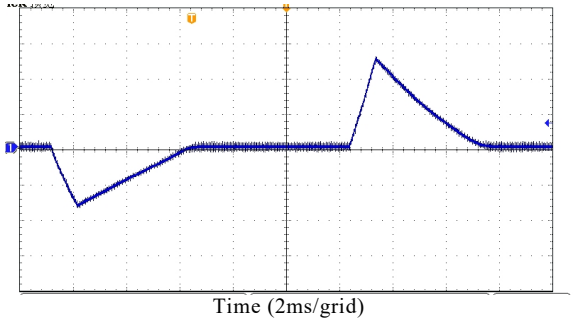

Time (2ms/grid)

Fig. 13. Experiment result of magnetic polarity identification for PMSynRM.

Figure 9 shows the space vector of classical three phase inverter. There are two pilot voltage vectors with same magnitude and opposite direction ($+V_{NS}$,$-V_{NS}$). When stator winding excited by two different pilot voltage vectors, the direction of flux generated by pilot voltage vector will be same or opposite with the flux generated by permanent magnet. Flux direction generated by permanent magnet and stator voltage pulse excitation was shown in Fig. 10. If the flux direction generated by pilot voltage is same with the flux of permanent magnet, the peak value of current response will be larger. This significant difference can be utilized to identify the polarity of rotor permanent magnet [10]. The explanation will be verified by experimental results in the following section.

VI. Experimental Results

Figure 11 shows comparison of estimated rotor position by high frequency signal injection and measured rotor position by sensor. Figure 12 shows comparison of estimated rotor position by sliding mode observer and measured rotor position by sensor. It can be seen that the error of estimated and measure rotor position signal is very small. It should be pointed out that the selection of injected frequency is a significant issue. If the frequency is too high, the magnitude of high frequency current will be too small, which resulted in difficulty to measure and filter out.

Figure 13 shows experimental result of rotor magnetic polarity identification. It is observed that the difference of peak value of current response can be measured to identify north or south polarity of additional rotor magnets. It should be point out that the magnitude or time duration of pilot voltage vector should be larger in order to cause the magnetic saturation effect and the difference of current magnitude can be detected easily.

VII. Conclusions

Sensorless control of ferrite permanent magnet-assisted synchronous reluctance machines over wide speed range using sliding mode observer and high frequency signal injection has been presented in this paper. The topology and feature of proposed ferrite permanent magnet-assisted synchronous reluctance machines have been introduced firstly. Sliding mode observer has been designed based on the dynamic model of proposed ferrite permanent magnet-assisted synchronous reluctance machines. The principles of high frequency signal injection and associated demodulation processes have been discussed. At standstill, a rotor polarity identification method has been proposed to

detect north or south pole. Finally, the experimental results show that the error of estimated rotor position and measured rotor position is very small. The rotor polarity can be detected by proposed scheme.

ACKNOWLEDGMENT

The author would like to thank Prof. Longya Xu (Department of Electrical and Computer Engineering, The Ohio State University, U.S.) for his discussions.

REFERENCES

[1] T. M. Jahns, G. B. Kliman, T. W. Eeumann, "Interior permanent magnet synchronous motors for adjustable-speed drive", *IEEE Trans. Ind Appl,* vol. 22, no. 4, pp. 738–747, 1986. [Online]. Available: http://dx.doi.org/10.1109/TIA.1986.4504786

[2] S. Morimoto, M. Sanada, Y. Takeda, "Performance of PM-assisted synchronous reluctance motor for high efficiency and wide constant power operation", *IEEE Trans. Ind. Appl.,* vol. 37, no. 5, pp. 1234–1240, 2001. [Online]. Available: http://dx.doi.org/10.1109/28.952497

[3] S. Ooi, S. Morimoto, M. Sanada, Y. Inoue, "Performance evaluation of a high-power-density PMASynRM with ferrite magnets", *IEEE Trans. Ind. Appl.*, vol. 49, no. 3, pp. 1308–1315, 2013. [Online]. Available: http://dx.doi.org/10.1109/TIA.2013.2253293

[4] M. Barcaro, N. Bianchi, F. Magnussen, "Permanent magnet optimization in permanent magnet-assisted synchronous reluctance motor for a wide constant power speed range", *IEEE Trans. Ind. Electronics.*, vol. 59, no. 6, pp. 2495–2502, 2012. [Online]. Available: http://dx.doi.org/10.1109/TIE.2011.2167731

[5] P. Niazi, H. A. Toliyat, D. H. Cheong, J. C. Kim, "A low cost permanent magnet-assisted synchronous reluctance motor drive", *IEEE Trans. Ind. Appl.,* vol. 43, no. 2, pp. 542–550, 2007. [Online]. Available: http://dx.doi.org/10.1109/TIA.2006.890033

[6] L. Jarzebowicz, "Indirect measurement of motor current derivatives in PMSM sensorless drives", *Elektronika Ir Elektrotechnika*, vol. 20, no. 7, pp. 23–26. [Online]. Available: http://dx.doi.org/10.5755/j01.eee.20.7.8019

[7] J. H. Jang, S. K. Sul, J. I. Ha, K. Ide, M. Sawamura, "Sensorless drive of surface-mounted permanent magnet motor by high frequency signal injection based on magnetic saiiency", *IEEE Trans. Ind. Appl.,* vol. 39, no. 4, pp. 1031–1039, 2003. [Online]. Available: http://dx.doi.org/10.1109/TIA.2003.813734

[8] J. H. Jang, J. I. Ha, M. Ohto, K. Ide, S. K. Sul, "Analysis of permanent magnet machine for sensorless control based on high frequency signal injection", *IEEE Trans. Ind. Appl.,* vol. 40, no. 6, pp. 1595–1604, 2004. [Online]. Available: http://dx.doi.org/10.1109/TIA.2004.836222

[9] J. Liu, T. A. Nondahl, P. B. Schmidt, S. Royak, M. Harbaugh, "Rotor position estimation for synchronous machines based on equivalent EMF", *IEEE Trans. Ind. Appl.*, vol. 47, no. 3, pp. 1310–1318, 2011. [Online]. Available: http://dx.doi.org/10.1109/TIA.2011.2125935

[10] J. Holtz, "Sensorless control of induction machines-with or without signal injection?", *IEEE Trans. Ind. Electronics.,* vol. 53, no. 1, pp. 7–30, 2006. [Online]. Available: http://dx.doi.org/10.1109/TIE.2005.862324

[11] J. Hu, J. Liu, L. Xu, "Eddy current effects on rotor position estimation and magnetic pole identification of PMSM at zero and low speeds", *IEEE Trans. Power Electronics.,* vol. 23, no. 5, pp. 2565–2575, 2008. [Online]. Available: http://dx.doi.org/10.1109/TPEL.2008.2002087